*Journal of Statistical Physics, Vol. 77, Nos. 3/4, 1994*

# Different Types of Self-Avoiding Walks on Deterministic Fractals

**Y. Shussman[1] and A. Aharony[1]**

*Received February 28, 1994; final April 21, 1994*

"Normal" and indefinitely-growing (IG) self-avoiding walks (SAWs) are exactly enumerated on several deterministic fractals (the Manderbrot–Given curve with and without dangling bonds, and the 3-simplex). On the $n$th fractal generation, of linear size $L$, the average number of steps behaves asymptotically as $\langle N \rangle = AL^{D_{saw}} + B$. In contrast to SAWs on regular lattices, on these factals IGSAWs and "normal" SAWs have the same fractal dimension $D_{saw}$. However, they have different amplitudes ($A$) and correction terms ($B$).

**KEY WORDS:** Self-avoiding walks; indefinitely-growing self-avoiding walks; fractals; renormalization.

## 1. INTRODUCTION

Random self-avoiding walks (SAWs) are often used as a model for polymer chains.[1] Some recent interest has concentrated on the statistics of SAWs on random substrates, and in particular on dilute networks.[2,3] Although it is now accepted that above the percolation threshold $p_c$, SAWs scale in the same way as in the nondilute case,[2] their behavior at this threshold is still open to research. At $p_c$, the spanning percolation cluster has fractal geometry.[3] Many aspects of this geometry have been successfully imitated by deterministic fractal structures[3] on which physical problems can be solved analytically. In this paper we solve the statistics of SAWs on several such fractal models.

There exist different types of SAWs, each having its own set of rules which define the weight associated with each SAW. The different types of walks can be basically divided into two groups:

[1] School of Physics and Astronomy, Raymond and Beverly Sackler Faculty of Exact Sciences, Tel Aviv University, Ramat Aviv 69978, Israel.



0022-4715/94/1100-0545$07.00/0 

1. *Kinetic walks*, in which the walk grows dynamically. For any time step there is a set probability for each possible direction (on a lattice) for the next step. This probability depends upon the history of this specific walk and can change from step to step. The total weight of the walk is the product of all the probabilities of the single steps.[4,5]

2. *Static walks*, in which a weight factor (denoted by $x$) is associated with each step of the SAW. The weight of an $N$-step SAW is $x^N$, disregarding the details of its path. SAWs which are forbidden accoding to the set of rules of this scheme have the weight factor zero.[6-8]

In this paper we focus upon two types of static SAWs. In both cases we limit ourselves to a fixed starting point, at the origin of a fractal generation, and consider SAWs which never visit any lattice site more than once. The first type of SAW is the indefinitely-growing SAW (IGSAW), in which a SAW is legitimate only if it is has the capability of continuing to grow forever from its present endpoint.[4,9] The second type is the "normal" SAW, which includes all possible SAWs whether or not they have the capability of further growth.

Previous papers[9,10] compared IGSAWs and SAWs on the two-dimensional square lattice. They used numerical simulations, in the canonical ensemble, and found the average end-to-end distance of the SAW $\langle R \rangle$ in terms of the number of steps $N$. The results were of the form $\langle R \rangle \sim N^{\nu}$, with $\nu = 1/D_{\text{saw}}$. They found a large difference between these two fractal dimensions ($\nu_{\text{SAW}} = 0.75$, while $\nu_{\text{IGSAW}} = 0.567$). They also suggested that the critical dimension for this problem was $d_c = 3$, and above it $\nu_{\text{SAW}} = \nu_{\text{IGSAW}}$.

The study of SAWs on regular lattices and on fractals has made much progress in the last two decades, using analytical and numerical methods. One of the methods which is most commonly used is the real-space renormalization group (RSRG) for a grand canonical ensemble of SAWs. Monte Carlo simulations using this approach were first handled by Render and Reynolds,[11] Berg and Forster,[12] and de Carvalho *et al.*[13] An analytical treatment for the problem using this method was first suggested by Dhar,[6] and by Rammal *et al.*,[7] who studied the problem of SAWs on fractals, and Shapiro,[8] who studied the problem on a triangular lattice. In the RSRG approach the problem is handled in the grand canonical ensemble, where a fugacity weight factor $x$ is associated with each step of the SAW. This yields a fixed point $x^*$ at which the SAW average length behaves as a power law $\langle N \rangle \sim L^{D_{\text{saw}}}$, where $L$ is the SAW end-to-end distance.

In this paper, we use RSRG to compare the masses, namely the average number of monomers $\langle N \rangle$, of the two types of SAWs on two different fractal structures. In order to do this, we define two kinds of ensembles. The first one is the grand-canonical ensemble, which contains all

the SAWs ("normal" or IGSAWs, depending on the problem) with a fixed end-to-end distance $R$ (this ensemble is used in the case of the 3-simplex). The second kind is a generalization of the grand-canonical ensemble, and it contains all the SAWs that start at the origin of a fractal generation of linear size $L$ and end at its edge or inside its bulk; therefore SAWs of various end-to-end distances (of order $L$ or smaller) are included in this ensemble (this generalization is used for the MG curve).

In contrast to the results obtained for the square lattice, we find that both IGSAWs and SAWs have the same $D_{saw}$ on a given fractal. However, we find a difference between the amplitudes of these two kinds of SAWs; the average number of monomers in the SAW $\langle N_S \rangle$ is larger than in the IGSAW $\langle N_I \rangle$. We also find correction terms to the expression for $\langle N \rangle$ in both cases, and these also depend on the type of SAW. Although our results were obtained only for two specific fractal structures, we have good reasons to believe that they are valid for all finitely ramified fractals, and hence also for percolation clusters at $p_c$.

The outline of our paper is as follows: Section 2 presents the two fractals (the Mandelbrot–Given curve and the 3-simplex). Section 3 introduces the RSRG, which is used as the analytical method. In Sections 4 and 5 we compare IGSAWs and SAWs on the MG curve and on the 3-simplex, respectively; Section 6 contains a discussion of finite-size corrections. Section 7 contains our conclusions.

## 2. THE FRACTALS

We chose to calculate $D_{saw}$ on two well-known fractal structures, which are basically different from each other. Two stages in their iterative construction are demonstrated in Fig. 1. The Mandelbrot–Given (MG)

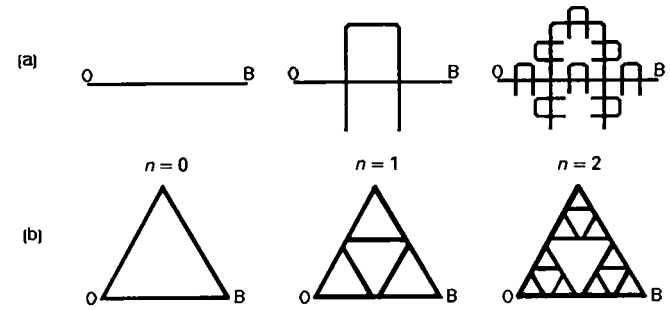


Fig. 1. First stages of iterative construction of fractal lattices ($n$ is the number of generations): (a) Mandelbrot–Given, (b) 3-simplex. $b$ is the length rescaling factor for each fractal. The short bonds in the 3-simplex are of negligible length. The edges of each fractal generation are denoted by $O$ and $B$. The distance between $O$ and $B$ is $L = b^n$.

curve[14] (Fig. 1a) is known to give a good qualitative and quantitative description of percolation clusters at $p_c$.[3] This is related to the fact that it contains blobs, nodes, links, and dangling ends, similar to our picture of these clusters.[15] For the fairness of comparison between the lengths of IGSAWs we made two kinds of calculations on the MG curve: we first chose to omit all the dangling ends (they are not accessible to the IGSAWs) and therefore we remain with the backbone of the MG curve; we then calculated the lengths of SAWs on the full MG curve (including the dangling ends) and found that there was only a minor difference in amplitudes between these two cases. The 3-simplex curve (Fig. 1b) is also a fractal of finite ramification which has also been used to imitate percolation clusters[6,16] with somewhat less quantitative success. [We note that the 3-simplex resembles the more familiar Sierpinski gasket (SG),[3,7] with the difference being that each pair of close vertices in the 3-simplex unite and the short bonds disappear in the SG. Therefore, a SAW on the 3-simplex can visit each vertex pair twice, a privilege which is denied for a SAW on the SG.]

## 3. THE ANALYTICAL METHOD

We define the free energy of a SAW on a fractal structure as follows.[17] Consider a fractal of the $n$th generation and linear size $L=b^n$ ($b=3$ for the MG curve, $b=2$ for the 3-simplex). We wish to study the behavior of a SAW on a deterministic environment, and therefore we assign an energy $\varepsilon$ for each bond. The statistical weight associated with each bond of the SAW is $x=\exp[-(\varepsilon-\mu)/kT]$, where $kT$ is the thermal energy and $\mu$ is the chemical potential per single bond. $x$ is sometimes called a "fugacity"[7] per single bond [in contrast to the usual definition of fugacity, $x=\exp(\mu/kT)$]. We choose to work in the grand-canonical ensemble, and therefore the partition function is the sum over all legitimate SAWs (depending on the type of SAW) of all lengths $N$ of the products of statistical weights

$$Z_n(x) \equiv \sum_{\text{SAWs}} x^N \tag{3.1}$$

where the boundary conditions for (3.1) are derived from our choice of what type of SAW is being averaged. Using the language of Section 1, we say that $Z_n$ is a partition function for all the static SAWs, and the weight factor associated with an $N$-step SAW is $x^N$. From the free energy $f_n = -kT \cdot \ln(Z_n)$ we can obtain the thermal average number of steps in the $n$th generation,

$$\langle N \rangle_n = -\frac{df_n}{d\mu} = \frac{x}{Z_n}\frac{dZ_n}{dx} \tag{3.2}$$

Our aim is to perform an exact calculation of $Z_n$ and $\langle N \rangle_n$. For this purpose we use the exact real-space renormalization group (RSRG) approach; knowing the value of $\langle N \rangle_n$, we calculate the value of the average number of steps $\langle N \rangle_{n+1}$ in the next generation. In our studied fractals, the iterative procedure by which those averages are calculated yields exact results. Since the average number of steps scales asymptotically as $\langle N \rangle \sim L^{D_{saw}}$, we have

$$D_{saw} = \lim_{n \to \infty} \frac{\ln(\langle N \rangle_{n+1} / \langle N \rangle_n)}{\ln(b)} \tag{3.3}$$

This method was first used by Rammal *et al.*[7] to determine the fractal dimension $D_{saw}$ of a SAW connecting the two edges of a fractal generation (in their notation $D_{saw} = 1/\nu$). $D_{saw}$ depends on the basic fugacity $x$, and they found that there was only one value of the critical fugacity $x_c$ for which the SAW was in a critical phase, so that its number of steps scaled like $\langle N \rangle \sim L^{D_{saw}}$. For $x > x_c$ the scaling is like $\langle N \rangle \sim L^{D_{max}}$ and the polymer is in the "compact" phase, while for $x < x_c$ $\langle N \rangle \sim L^{D_{min}}$ and the polymer is in the "extended" phase ($D_{min}$ and $D_{max}$ are the fractal dimensions of the shortest and the longest SAWs on the fractal, respectively). Using the language of the renormalization group, we say that the polymer is in the critical phase when the initial fugacity is at the fixed point $x = x^*$. Any initial value of the fugacity which is different from $x^*$ causes the expression on the right-hand side of (3.3) to approach $D_{max}$ or $D_{min}$ as $n$ goes to infinity (Fig. 2).

In ref. 7, the polymer had both ends fixed at the edges of a fractal generation ($O$ and $B$ in Fig. 1). This implicitly assumed that the polymer is of the type of the IGSAW; all the SAWs that could not reach the edge of this fractal generation were excluded from the partition function (3.1).

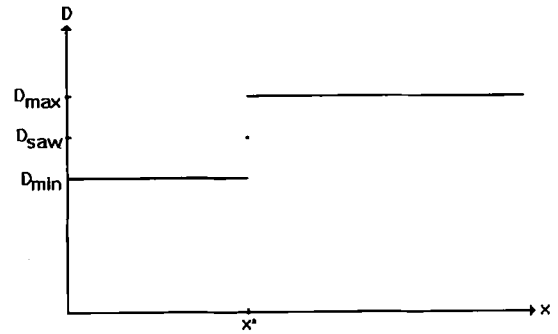


Fig. 2. Dependence of the fractal dimension of a SAW on the fugacity.

Moreover, there are many IGSAWs that are excluded from (3.1) because they actually end inside the bulk of a fractal generation. In the next section we generalize the results of ref. 7 for the two cases of IGSAWs that end inside the bulk of a fractal generation and of "normal" SAWs.

## 4. SAWs ON THE MANDELBROT–GIVEN (MG) CURVE

### 4.1. The Fixed Point

We define a partial partition function $E_n(x)$ which contains all the terms that arise from SAWs that start at the origin ($O$ in Fig. 1a) and reach the other end ($B$ in Fig. 1a) of the $n$th generation. A SAW of the $(n+1)$th generation can choose its way by either taking the short path (in which it passes through 3 $n^{\text{th}}$-generations) or take the long path (5 $n^{\text{th}}$-generations). Therefore, following the method of ref. 7, we write

$$E_0 = x, \qquad E_{n+1} = E_n^3 + E_n^5 \tag{4.1a}$$

where the partition function $E_n$ contains all the possibilities to pass through the $n$th generation from the origin to its end. In the language of the renormalization group we can define $E' \equiv E_{n+1}$ and $E \equiv E_n$ and rewrite (4.1a)

$$E' = E^3 + E^5 \tag{4.1b}$$

This recursion relation has three fixed points (where $E' = E$), i.e., $E = 0$, $E^*$, $\infty$. At the nontrivial fixed point $E^*$ the polymer resembles itself on any scale (in the sense that its rescaling factor does not depend on the number of generations $n$), and this identifies its "critical" phase. We can now substitute the initial condition $E_0 = x$ into the recursion relation (4.1b) and come out with an equation for the fugacity's fixed point $x^*$,

$$x^* = x^{*3} + x^{*5} \tag{4.2}$$

whose nontrivial solution is $x^* = E^* = [(\sqrt{5}-1)/2]^{1/2} = 0.7862\ldots$. The fractal dimension of the SAWs that are included in $E_n$ depends on the derivative $m = dE'/dE|_{E^*} = 3x^{*2} + 5x^{*4} = 6 - \sqrt{5} = 3.7639\ldots$. At the fixed point[7]

$$D_{\text{saw}} = \frac{\ln(m)}{\ln(3)} = 1.2065 \tag{4.3}$$

An exact expression for the average number of monomers $\langle N_E \rangle_n$ in a SAW on the fractal $n$th generation is found by substituting the partition

function $E_n$ into Eq. (3.2). At the fixed point $E_n = E^* = x^*$ this yields an iterative equation whose solution is exactly[7]

$$\langle N_E \rangle_n = m^n = 3^{n \cdot D_{\text{saw}}} \equiv L^{D_{\text{saw}}} \tag{4.4}$$

Thus, the amplitude of the edge-to-edge SAWs on the MG curve is exactly equal to 1, and there are no corrections to the pure power law.

Looking at Fig. 2, it is obvious that any value of initial fugacity which is different from $x^*$ will be dominated by the $E^5$ or the $E^3$ terms in Eq. (4.1b), and will thus yield $D_{\max} = \ln(5)/\ln(3)$ or $D_{\min} = 1$. Therefore, from now on we will analyze the fractal dimension at $x^*$.

## 4.2. IGSAWs on the MG Curve

The grand-canonical ensemble, which is used to obtain the fractal dimension of the edge-to-edge SAW on the MG curve, becomes unsuitable when one wants to analyze the properties of a SAW which does not end at an edge of a fractal generation. Therefore we define an IGSAW ensemble which is a generalization of the grand-canonical ensemble; for a lattice of linear size $L$, the ensemble contains all the IGSAWs that start at the edge of a fractal generation and end inside its bulk or at its other edge. Therefore, all the IGSAWs that are included in this ensemble have an end-to-end distance which is smaller than or equal to $L$. Note that all of these IGSAWs only visit the backbone of the structure, and not its dangling ends. Following this, the partition function $I_1(x)$ for the IGSAWs on the first generation of the lattice is (see Fig. 3)

$$I_1(x) = x + 2x^2 + 2x^3 + x^4 + x^5 \tag{4.5}$$

We can iteratively write $I_{n+1}(x)$ for any generation $n+1$ as a function of $I_n(x)$ and $E_n(x)$ (see Fig. 3)

$$\begin{aligned} I_{n+1}(x) &= I_n + 2E_n I_n + 2E_n^2 I_n + E_n^3 I_n + E_n^4 I_n \\ &= \frac{I_n(x)}{E_n(x)} I_1(E_n(x)) \end{aligned} \tag{4.6}$$

It should be noted that once we set $E_n$ to be equal to $E^*$, $I_n$ does not have a finite-value fixed point, and if we look for such a point we would only

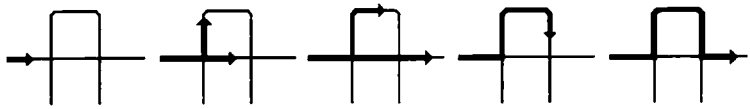

Fig. 3. IGSAWs of the $n+1$ generation as a function of $n$th-generation IGSAWs on the MG curve.

find the nonphysical solution $I^*=0$ or $I^*=\infty$. This is a direct consequence of our definition of the IGSAW ensemble: it includes all the IGSAWs that end inside the bulk of the $n$th generation, and therefore $I_{n+1}$ contains all the IGSAWs that are included in $I_n$, plus many others. Therefore as $n$ grows, $I_n$ diverges.

Applying Eq. (3.2) to $I_{n+1}$ results in an iterative expression for the average of all IGSAWs in the $n+1$ generation,

$$\langle N_I\rangle_{n+1}=\frac{x}{I_{n+1}(x)}\frac{d}{dx}\left[\frac{I_n(x)}{E_n(x)}I_1(E_n(x))\right] \tag{4.7}$$

and a straightforward calculation, using (3.2) and remembering that at the fixed point of the fugacity $E_n(x^*)=x^*$ for every $n$, yields

$$\langle N_I\rangle_{n+1}=\langle N_I\rangle_n+(\langle N_I\rangle_1-1)\frac{dE_n(x)}{dx} \tag{4.8}$$

The iterative equation (4.8) can be solved as follows: Using $m=dE_n(x)/dE_{n-1}|_{x^*}$ and Eq. (4.3) yields

$$\frac{dE_n}{dx}=\frac{dE_n}{dE_{n-1}}\frac{dE_{n-1}}{dE_{n-2}}\cdots\frac{dE_1}{dx}=m^n \tag{4.9}$$

with $m=3^{D_{\text{saw}}}$. Substituting (4.9) into (4.8) yields

$$\langle N_I\rangle_{n+1}=\langle N_I\rangle_n+(\langle N_I\rangle_1-1)\,m^n \tag{4.10a}$$

$$=\langle N_I\rangle_1+\sum_{i=1}^{n}(\langle N_I\rangle_1-1)\,m^i \tag{4.10b}$$

$$=\frac{\langle N_I\rangle_1-1}{m-1}m^{n+1}+\frac{m-\langle N_I\rangle_1}{m-1} \tag{4.10c}$$

where (4.10b) was derived by substituting (4.10a) iteratively into itself. The right term of (4.10c) is a constant. Since $m>1$, the left term there immediately yields the fractal dimension of the IGSAW on the MG curve,

$$D_{\text{saw}}(\text{IGSAW})=\ln(m)/\ln(3)=1.2065... \tag{4.11}$$

i.e., the same value as in the case of edge-to-edge SAWs [Eq. (4.3)].

Using Eq. (4.7) for $n=0$ at $x^*$, we find $\langle N_I\rangle_1=2.5033...$. Therefore,

$$\langle N_I\rangle_n=0.5439m^n+0.4561=0.5439L^{D_{\text{saw}}}+0.4561 \tag{4.12}$$

where the right term in (4.12) is a constant correction (and therefore of the order $1^n=L^0$).

We should emphasize that the fractal dimension of the IGSAW found here is equal to that found by Rammal *et al.*[7] In our notation, what they found was the dimension of all the SAWs included in the partition function $E_n$.

The difference in amplitudes between (4.4) and (4.12) can be qualitatively explained as follows: (4.4) is an average of only a part of the SAWs that are averaged in (4.12); all the SAWs averaged in (4.4) reach the edge of the $n$th generation and are therefore generally longer compared to the SAWs averaged in (4.12). This is the reason for the amplitude in (4.4) being larger than that in (4.12).

## 4.3. SAWs on the MG Curve

Let us now use the same procedure to determine the fractal dimension of the "normal" SAWs. As we noted earlier, we first discuss those SAWs that do not enter the dangling ends and therefore travel only on the backbone of the fractal.

The ensemble is defined similarly to Section 4.2, and contains all the SAWs that start at the edge of a fractal generation and end inside its bulk or at its other edge. We introduce an auxiliary partition function $C_n(x)$, which includes all the terms arising from SAWs which are restricted to the $n$th generation but do not reach its edge. We also define the total partition function $S(x)$, which includes all the terms of all the SAWs in the ensemble, hence $S_n(x) = C_n(x) + E_n(x)$, where $E_n(x)$ was defined earlier. The initial partition functions are (see Fig. 4)

$$\begin{aligned} C_1(x) &= x + 2x^2 + 2x^3 + 2x^4 \\ S_1(x) &= x + 2x^2 + 3x^3 + 2x^4 + x^5 \end{aligned} \tag{4.13}$$

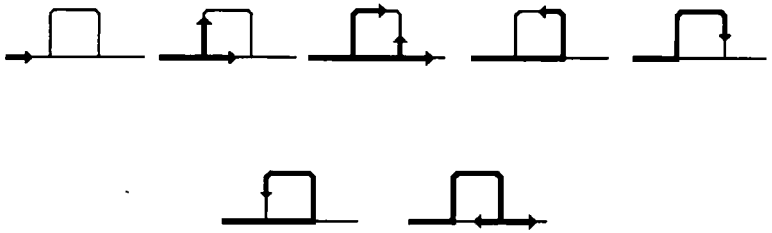

Fig. 4. SAWs of the $n+1$ generation as a function of $n$th-generation SAWs on the backbone of the MG curve; see Eqs. (4.13) and (4.14).

Iterative construction of the partition function $S$ for the $n+1$ generation yields (see Fig. 4)

$$S_{n+1}(x) = \{S + 2ES + 3E^2S + 2E^3S + E^4S + 2E^4C\}_n \tag{4.14a}$$

$$= \frac{S_n(x)}{E_n(x)} S_1(E_n(x)) + 2E_n^4(x)\, C_n(x) \tag{4.14b}$$

where the index $n$ on the curly brackets in (4.14a) refers to each of the partition functions inside.

We could now follow the same procedure which we used after Eq. (4.6), to determine the fractal dimension of the SAWs, but there is one major difference between (4.6) and (4.14b); the right term in (4.14b) prevents us from proceeding in the same way as in (4.7) [the terms do not cancel after taking the derivative and we cannot reach an expression similar to (4.8)]. Therefore we have to use a different procedure, and we start by applying (3.2) to (4.14b) and write a recursion relation for the average length of the SAW,

$$\langle N_S \rangle_{n+1} = \frac{x}{S_{n+1}} \left[ \frac{\alpha S_n}{x} \langle N_S \rangle_n + (\beta S_n - 10E_n^4)\, m^n \right] \tag{4.15}$$

where $\alpha = 1 + 2E_n + 3E_n^2 + 2E_n^3 + 3E_n^4$, $\beta = d\alpha/dE_n$, and $m = dE'(x^*)/dE$. Remembering that at the fixed point $E_n = x^*$ for all $n$, the three terms $\alpha$, $\beta$, and $m$ are all constants. We can now substitute into (4.15) a simplified version of (4.14a),

$$S_{n+1} = \alpha S_n - 2x^{*5} \tag{4.14c}$$

A straightforward calculation then yields

$$\langle N_S \rangle_{n+1} = \left(1 + \frac{2x^{*5}}{S_{n+1}}\right) \langle N_S \rangle_n + \frac{\beta x^* S_n - 10x^{*5}}{S_{n+1}} m^n \tag{4.16}$$

At the fixed point, $\alpha = 6.5440...$; therefore, as $n$ goes to infinity, $S_n$ diverges geometricaly. We can express the value of $S_n$ at the fixed point by substituting (4.14c) into itself and obtaining

$$S_n = \alpha^{n-1} \left(S_1 - \frac{2x^{*5}}{\alpha - 1}\right) + \frac{2x^{*5}}{\alpha - 1} \tag{4.17}$$

Substituting (4.17) into (4.16) and omitting all the terms that tend to zero in the limit $n \to \infty$ then yields

$$\langle N_S \rangle_{n+1} = \langle N_S \rangle_n + \frac{\beta x^*}{\alpha m} m^{n+1} + \text{corrections} \tag{4.18}$$

Substituting (4.18) iteratively into itself yields the leading-order expression

$$\langle N_S \rangle_n \approx \frac{\beta x^*}{\alpha(m-1)} m^n + \left(1 - \frac{\beta x^*}{\alpha(m-1)}\right) = 0.7065 m^n + c \qquad (4.19)$$

Although (4.19) implies the existence of a constant correction term $c$, the value of $c$ there is meaningless because it was calculated to match the initial condition $n=0$ instead of the asymptotic behavior at $n \to \infty$. The value of $c$ can be calculated numerically by iterating (4.16) and comparing the results for every $n$ to (4.19). After about $n \sim 15$ iterations $\langle N_S \rangle_n$ stabilizes to the form (4.19), with $c = -0.4056\ldots$.

A better approximation is found by noting that in the limit $n \to \infty$, $S_n$ scales like $S_n \sim \alpha^n$. We now take a perturbation theory approach and substitute the first-order solution (4.18) into the exact recursion relation (4.16). Doing this and using (4.17) yields the second-order correction

$$\begin{aligned} \langle N_S \rangle_n &\approx 0.7065 m^n - 0.4056 + 0.7461 \left(\frac{m}{\alpha}\right)^n \\ &= 0.7065 L^{D_{\text{saw}}} - 0.4056 + 0.7461 L^{-x} \end{aligned} \qquad (4.20)$$

where $x = \ln(\alpha/m)/\ln(3) = 0.5034\ldots$.

Since $m/\alpha < 1$, the third term in (4.20) is irrelevant and the approximation (4.19) is valid for large $L$. Higher corrections involve larger powers of $(m/\alpha)^n$.

Comparing the average (4.19) of the SAWs to the average (4.12) of the IGSAWs shows an identity of the fractal dimension $D_{\text{saw}} = \ln(m)/\ln(3)$ and a difference in the amplitude. Moreover, the only relevant parameter which determines the fractal dimension in both cases is $m = dE'/dE|_{x^*}$, which is connected through its definition only to the paths reaching the edge of a fractal generation. This result can be intuitively explained as follows: due to the singly connected bonds in the MG curve, a SAW is really non-indefinitely growing only from a certain point at which it makes a "mistake" and enters a blob from which it cannot get out. Until reaching this point the walk is practically indefinitely growing, and this explains the identity of the fractal dimensions. However, there is some difference in the average lengths of these two walks, and this is reflected in the amplitude, which (as expected) is larger for the SAWs.

A similar procedure to that used in this section can be carried out for the SAWs that can enter the dangling ends. In order to proceed with the calculation for this case, straightforward modifications have to be introduced into the initial partition function (4.13) and into the recursion relation (4.14). The leading term of the final result for this case is

$$\begin{aligned} \langle N_S \rangle_n &= 0.7092 m^n + O\{1^n\} \\ &= 0.7092 L^{D_{\text{saw}}} (1 + O\{L^{-D_{\text{saw}}}\}) \end{aligned} \qquad (4.21)$$

The difference between the amplitudes of (4.20) and (4.21) arises only from the difference in $\beta$ for the two cases. This result shows only a minor difference with respect to (4.20), and therefore implies that the dangling ends do not play a significant role in determining the average length of a SAW. The intuitive explanation for this is that adding the dangling ends creates a large number of new SAWs, some of which are shorter than the average SAW, and others which are longer. The calculation yields, however, that the average SAW changes only slightly due to the addition of the dangling ends.

## 5. SAWs ON THE 3-SIMPLEX (3S) CURVE

### 5.1. The Types of SAWs on the 3S Curve

In view of the results of Section 4.2, it looks interesting to examine IGSAWs and SAWs on a fractal curve of a different type. We chose the 3-simplex for its lack of singly connected bonds; this fact enables a SAW starting at the origin to be of arbitrary length (on the MG curve this kind of SAW has a bounded length). Therefore there might be a difference in the fractal dimensions between these two types of SAW.

On the MG curve we examined the dependence of the SAW average length $\langle N \rangle$ on the lattice linear size $L$. In the case of the 3S curve we make a slight modification and examine the dependence of $\langle N \rangle$ on the SAW end-to-end distance $R = b^n$ in the grand-canonical ensemble ($b = 2$ in the 3S). Using Fig. 5, we define all the SAWs to start at the origin $O$ and end at $B$, which is the edge of the $n$th fractal generation. We now define the following partition functions: (a) $E_n$ for all the SAWs that may visit $A$, but do not exit through $A$ and therefore are restricted to the boundaries of the $n$th generation (Fig. 5a), (b) $I_n$ for all the SAWs that reach $B$ and are indefinitely growing from there, irrespective of whether they exit through $A$ or not (Fig. 5b), and (c) $S_n$ for all the SAWs that end at $B$, irrespective of being an IGSAW or not (Fig. 5c). This modification would have no meaning if it was made with respect to the MG curve; but due to the ability of a SAW on the 3S to exit at one generation and to return at a later stage, it is meaningful here. Another projection of this modification, which will be shown later, is that in contrast to the case of SAWs on the MG curve, both partition functions $I_n$ and $S_n$ do have finite fixed-point values.

We start by stating the results of ref. 7 concerning the fractal dimension of the SAWs included in $E_n$. The initial partition function for the

zeroth generation includes both possible ways to carry out an end-to-end SAW (Fig. 2b),

$$E_0 = x + x^2 \tag{5.1a}$$

and the recursion relation for higher generations is

$$E_{n+1} = E_n^2 + E_n^3 \tag{5.1b}$$

Using the renormalization group notation $E \equiv E_n$ and $E' \equiv E_{n+1}$, (5.1) transforms into the expression $E' = E^2 + E^3$. The fixed point $E^*$ satisfies the equation $E' = E$ with the solution $E^* = (\sqrt{5} - 1)/2 = 0.6180$. The initial condition (5.1a) defines an equation for $x^*$, $x^* + x^{*2} = E^*$, with the

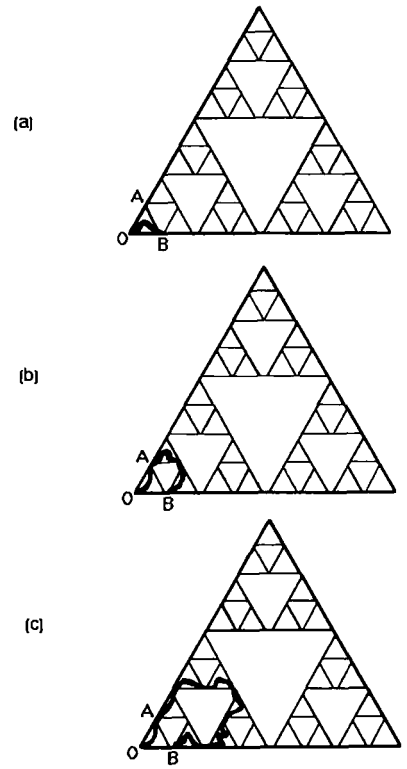


Fig. 5. Examples of SAWs on the 3-simplex. $OAB$ is the $n$th generation: (a) The SAW does not exit through $A$. (b) The SAW exits through $A$, returns to $B$, and is indefinitely growing from $B$. (c) The SAW exits through $A$, returns to $B$, and is not indefinitely growing.

solution $x^* = 0.4317$. Using Eq. (3.2), a straightforward calculation yields the average number of steps

$$\langle N_E \rangle_n = \langle N_E \rangle_0 m^n \tag{5.2a}$$

where

$$\langle N_E \rangle_0 = \frac{x^* + 2x^{*2}}{E^*} = 1.3015, \quad m = \left.\frac{dE'}{dE}\right|_{E^*} = 2E^* + 3E^{*2} = 2.3820... \tag{5.2b}$$

The fractal dimension of these SAWs is $D_{\text{saw}}(E) = \ln(m)/\ln(2) = 1.2522...$, somewhat higher than our MG result.

## 5.2. IGSAWs on the 3S Curve

We are now able to treat the average length of IGSAWs. The ensemble of all such $n$th-generation possible walks between $O$ and $B$ is bounded in the dashed area of Fig. 6 and therefore satisfies the partition function

$$I_n = E_n + E_n^2 E_{n-1} E_{n-2} \cdots E_1 E_0 x \tag{5.3a}$$

We can use the case of $n = 1$ as an example for Eq. (5.3). In this case, an IGSAW starts from point $O$ of Fig. 6 and ends at $B$. It can either take the short path from $O$ to $B$ (without exiting through $A$), or take a path passing through $A$ and $C$. In the latter case, the SAW is forbidden to visit point $D$ in order to remain indefinitely growing. Therefore the partition function for the IGSAWs of the first generation is

$$I_1 = E_1 + E_1^2 E_0 x \tag{5.3b}$$

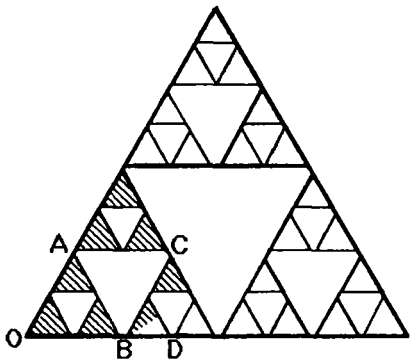


Fig. 6. The dashed area indicates all possible IGSAWs starting at the origin $O$ and ending at the edge $B$ of the $n$th generation. The half-filled triangle indicates that the IGSAW is forbidden to visit point $D$.

where the left term satisfies the short path and the right term satisfies all the possible long paths.

We can now self-consistently rewrite (5.3a)

$$I_{n+1} = E_{n+1} + E_{n+1}^2 E_n E_{n-1} \cdots E_1 E_0 x$$
$$= E_{n+1} + \frac{E_{n+1}^2}{E_n}(I_n - E_n) \tag{5.4}$$

and examine the partition function $(I-E)$. This function includes all the terms arising from IGSAWs that leave the $n$th generation via $A$ and return later on to $B$. Following (5.4), $(I-E)$ obeys the recursion relation

$$(I-E)_{n+1} = \frac{E_{n+1}^2}{E_n}(I-E)_n \tag{5.5}$$

At the fixed point $E_n = E^*$ the prefactor becomes $E^* < 1$, and thus $I_n$ flows toward the fixed point $I^* = E^*$. Applying the average calculation procedure (3.2) to (5.5) reduces to

$$\langle N_{I-E}\rangle_{n+1} = \langle N_{I-E}\rangle_n + 2\langle N_E\rangle_{n+1} - \langle N_E\rangle_n \tag{5.6}$$

Using (5.2) and then substituting (5.6) recursively into itself yields

$$\langle N_{I-E}\rangle_n = \frac{\langle N_E\rangle_0 (2m-1)}{m-1} m^n + \left[\langle N_{I-E}\rangle_0 - \frac{(2m-1)\langle N_E\rangle_0}{m-1}\right]$$
$$= 3.5448 m^n + 0.0582 = 3.5448 R^{D_{\text{saw}}} + 0.0582 \tag{5.7}$$

where $\langle N_{I-E}\rangle_0$ was calculated using the partition function obtained from (5.3a), $(I-E)_0 = E_0^2 x$.

It is now possible to obtain the desired average $\langle N_I\rangle_n$ using the weighted average formula

$$I\langle N_I\rangle = (I-E)\langle N_{I-E}\rangle + E\langle N_E\rangle \tag{5.8}$$

Using (5.2), (5.3), and (5.7), we find

$$\langle N_I\rangle_n = 1.3015 m^n + 0.5986 (E^* m)^n + O\{(E^{*2} m)^n, (E^*)^n\}$$
$$= 1.3015 R^{D_{\text{saw}}}(1 + 0.4599 R^{-0.6942} + O\{R^{-1.3884}, R^{-1.9465}\}) \tag{5.9}$$

We now compare the average (5.9) of all the IGSAWs to the average (5.2) of the SAWs that are restricted to within the boundaries of the $n$th generation. They both have the same leading term, including the length rescaling factor and the amplitude. This equality of the leading terms in both cases

can be explained by fact that asymptotically $I^* = E^*$; thus, the term which involves $(I-E)$ in Eq. (5.8) and expresses the weight of the longer paths does not contribute to the average length in the first order. Thus the fractal dimensions for both ensembles are identical and equal to $D_{saw}(I) = D_{saw}(E) = \ln(m)/\ln(2) = 1.2522....$

## 5.3. "Normal" SAWs on the 3S Curve

Consider now the case of SAWs on the 3S curve, which is presented in Fig. 7. A SAW with $R = 2^n$ steps end-to-end distance starts at the origin $O$ and ends at $B$ ($OAB$ is the $n$th generation). The SAW can choose its way from $O$ to $B$ among all the combinations presented in Fig. 7. Due to the infinite size of the lattice, the number of such combinations is also infinite.

Following this, the partition function for the SAWs is

$$\begin{aligned} S_n &= E_n + E_n^3 + E_n^3 E_{n+1}^2 + E_n^3 E_{n+1}^2 E_{n+2}^2 + \cdots \\ &= E_n \left[ 1 + \sum_{k=n}^{\infty} \prod_{i=n}^{k} E_i^2 \right] \equiv E_n \cdot G \end{aligned} \tag{5.10}$$

where $G$ denotes the contents of the brackets.

Substituting the value of the fixed point $E = E^*$ into (5.10), we see that the series converges for all $n$ to $S_n = 1$; therefore the function $S_n$ has a fixed value $S = S^* = 1$. By using Eq. (3.2) and substituting this value, we can express $\langle N_S \rangle_n$ by

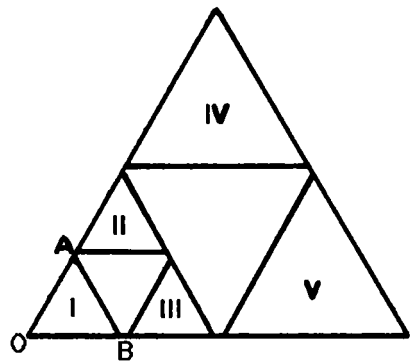


Fig. 7. SAWs from $O$ to $B$ on the 3-simplex. The SAW can choose one of the following combinations: {I}, {I, II, III}, {I, II, IV, V, III}, and so on (the lattice is infinite). $OAB$ represents the $n$th generation.

$$\langle N_S \rangle_n = xG \frac{dE_n}{dx} + xE_n \frac{dG}{dx}$$

$$= \frac{xS_n}{E_n} \frac{dE_n}{dx} + xE_n \sum_{k=n}^{\infty} \sum_{j=n}^{k} \frac{2}{E_j} \frac{dE_j}{dx} \prod_{i=n}^{k} E_i^2 \tag{5.11}$$

Now we can substitute into (5.11) the fixed-point values for all $n$, $E_n = E^*$, and $S_n = 1$, and the chain derivative $dE_j/dx = m^j \, dE_0/dx$ [$m$ was defined in (5.2)]. The result involves two composed geometrical series, yielding

$$\langle N_S \rangle_n = \frac{(E^* + E^{*3}) \langle N_E \rangle_0}{1 - mE^{*2}} m^n = 12.329 m^n = 12.329 R^{D_{saw}} \tag{5.12}$$

with no corrections. Comparing the averages of the IGSAWs and SAWs again shows an identity in the fractal dimensions but a great difference in the amplitude, which, as expected, is much larger for the SAWs.

## 6. CORRECTIONS DUE TO FINITE-SIZE EFFECTS

An ideal fractal contains an infinite number of generations. However, when one wants to establish theoretical predictions for experimental results (or for computer simulations) one must take into account the effects generated due to the finite size of the sample, whose length characteristics are bounded between the lattice parameter $a$ and its linear size $L$. These finite-size effects are relevant in only one of the cases that were discussed earlier; this is the case of SAWs in the 3S. In all the other cases there is no influence of such effects, because the SAW is restricted to a small portion of the lattice (on the MG curve an $n$-generation SAW cannot exit the $n$th generation, and on the 3S an $n$-generation IGSAW cannot exit the $(n+1)$th generation).

Consider $N$ generations of the 3S lattice, with a linear size $L = 2^N$. A SAW with the end-to-end-distance of $R = 2^n$ travels on this lattice from the origin to the edge of the $n$th generation. The case of interest is for $n \ll N$; otherwise, the SAW is restricted to a portion of the lattice $L \sim R$.

The calculation for this case is done by cutting the series $G$ in (5.10) after the $(N-1)$th term and obtaining the finite-size partition function $S_n^N$. The average $\langle N_S^N \rangle_n$ is then calculated using Eq. (3.2),

$$\langle N_S^N \rangle_n = \frac{x}{S_n^N} \frac{dS_n^N}{dx} = \langle N_E \rangle_n + \frac{xE^*}{1 - E^{*2(N-n+1)}} \frac{dG}{dx} \tag{6.1}$$

After a heavy but straightforward calculation similar to the one presented in Section 5, we find the derivative $dG/dx$,

$$\frac{dG}{dx} = \frac{2\langle N_E \rangle_0}{x^*(m-1)} \left(\frac{1}{E^{*2}}\right)^n \left[ m \frac{(mE^{*2})^N - (mE^{*2})^n}{mE^{*2}-1} - m^n \frac{E^{*2N} - E^{*2n}}{E^{*2}-1} \right] \quad (6.2)$$

Substituting (6.2) into (6.1) in the limit $n \ll N$, we obtain the leading finite-size corrections terms

$$\begin{aligned} \langle N_S^N \rangle_n &= 12.329 m^n - 11.725 (mE^{*2})^N \left(\frac{1}{E^{*2}}\right)^n + O(m^n E^{*2N-2n}) \\ &= 12.329 R^{D_{\text{saw}}} \left[ 1 - 0.951 \left(\frac{R}{L}\right)^{0.1363} + O\left\{ \left(\frac{R}{L}\right)^{1.3886} \right\} \right] \end{aligned} \quad (6.3)$$

The correction terms in (6.3) contain a positive power of $R$, but their amplitude decays to zero in the limit $R \ll L$.

## 7. DISCUSSION AND CONCLUSIONS

We established that the three types of SAW (edge-to-edge, IGSAW, and SAW) on the same fractal have the same fractal dimensions. Although the fractals that were examined were basically different from one another, the final expression for the SAW average length had the same exponent in all the cases, and the differences appeared in amplitudes and correction terms.

We found the exact amplitudes for three types of SAWs (E, IGSAW, and SAW) on two fractals (Mandelbrot–Given curve and 3-simplex). We showed that there is a basic difference in the relations between the amplitudes in these two fractals: In the MG curve, the singly-connected bonds prevent the SAW from reentering a generation which it previously left; this causes the edge-to-edge SAWs to be the longest and the indefinitely-growing SAWs, which can end inside the bulk, to be the shortest. Therefore the relation between the amplitudes is $A(E) > A(\text{SAW}) > A(\text{IGSAW})$. In contrast, on the 3-simplex, a SAW can travel to infinity and then return to an ending point very close to its starting point. This causes the relation between the amplitudes to be $A(\text{SAW}) > A(\text{IGSAW}) = A(E)$, where $A(\text{SAW})$ is significantly larger than the other two amplitudes.

Our results show a major difference in the properties of IGSAWs on fractals with respect to regular lattices, as obtained in refs. 9 and 10. Following Vannimenus,[18] we suggest that this can be an outcome of the topological constraint which is common for both of our fractals, that a SAW can only enter once an $n$th-generation iteration. This constraint does

not exist, however, on other fractals, such as the 3-dimensional Sierpinski gasket or the 3-dimensional 3-simplex. It will therefore be most interesting to carry out an analysis similar to the one presented here for these fractals.

It is widely agreed that the MG curve represents an excellent model for the infinite percolation cluster at $p_c$.[3] Therefore, there is reason to expect that a polymer's fractal dimension in a dilute system at $p_c$ is independent of the type of SAW. The difference between average lengths of different types of polymers on such a cluster appears only through the amplitudes and correction terms. It would be interesting to test these predictions on real percolation clusters.

## ACKNOWLEDGMENTS

This paper was supported by the Israel Academy of Sciences and Humanities, the U.S.–Israel Binational Science Foundation (BSF) and by the German–Israeli Foundation (GIF).

## REFERENCES

1. P. G. de Gennes, *Scaling Concepts in Polymer Physics* (Cornell University Press, Ithaca, New York, 1979).
2. A. B. Harris, *Z. Phys. B* **49**:347 (1983).
3. D. Stauffer and A. Aharony, *Introduction to Percolation Theory* (Taylor & Francis, London, 1992). Revised 2nd edition, 1994.
4. A. Coniglio, N. Jan, I. Majid, and H. E. Stanley, *Phys. Rev. B* **35**:3617 (1987).
5. R. M. Ziff, *Physica D* **38**:377 (1989).
6. D. Dhar, *J. Math. Phys.* **19**(1):5 (1978).
7. R. Rammal, G. Toulouse, and J. Vannimenus, *J. Phys.* (Paris) **45**:389 (1984).
8. B. Shapiro, *J. Phys. C: Solid State Phys.* **11**:2829 (1978).
9. K. Kremer and J. W. Lyklema, *Phys. Rev. Lett.* **54**:267 (1985).
10. K. Kremer and J. W. Lyklema, *J. Phys. A* **18**:1515 (1985).
11. S. Redner and P. J. Reynolds, *J. Phys. A* **14**:2679 (1981).
12. B. Berg and D. Forster, *Phys. Lett.* **106B**:323 (1981).
13. C. A. de Carvalho and S. Caracciolo, *J. Phys.* (Paris) **44**:323 (1983).
14. B. B. Mandelbrot and J. A. Given, *Phys. Rev. Lett.* **52**:1853 (1984).
15. H. E. Stanley, *J. Phys. A* **10**:L211 (1977).
16. Y. Gefen, A. Aharony, B. B. Mandelbrot, and S. Kirkpatrick, *Phys. Rev. Lett.* **47**:1771 (1981).
17. P. Le Doussal and J. Machta, *J. Stat. Phys.* **64**:541 (1991).
18. J. Vannimenus, *Physica D* **38**:351 (1989).